

MECHANICAL DESIGN OF A PROTON CIRCULAR ACCELERATOR FOR THERAPY PURPOSES

Luísa de Araújo Rabelo¹

Tarcísio Passos Ribeiro de Campos²

Universidade Federal de Minas Gerais – Av. Antônio Carlos 6627 – Pampulha /MG

¹ luisarabelo88@gmail.com, ² tprcampos@pq.cnpq.br

Abstract. Proton radiation therapy has been applied to the solid tumor showing control in most cases with less deleterious effects. The protons have higher energy deposition in depths with reduced lateral spread, compared to photons and electrons beams, with suitable characteristic energy deposition peak (Bragg peak). For this technique is required large particle accelerators which hinders the implementation of Proton Therapy Centers in Brazil, due to the needs for investments of tens of millions of dollars. This study addresses a new project of an electromagnetic unit based on a proton circular acceleration able to attach to national radiopharmaceutical-producer cyclotrons, of 15MeV, to meet the 65MeV energies required to eye-therapy. Herein, there were evaluated physical parameters of the proton beam, through classical and relativistic mechanics formulations; simulations based on ion electromagnetic field transport in EMF CST (Computer Simulation Technology); and equipment modeling using AutoCAD. The structure is differentiated from other circular accelerators (patent CTIT/UFMG-NRI research group/UFMG). The results show the major parameters of the project as well as its technical design. As conclusion, there is a viability of developing compact equipment running isolated as gun accelerator or post accelerator for cyclotrons to provide proton therapy in Brazil. The reducing costs of manufacture, installation and operation of this equipment will facilitate the dissemination of this treatment in Brazil and consequently advancing in fighting cancer.

Keywords: Circular, Accelerator, Protons, Therapy, Compact.

1. INTRODUCTION

Charged elementary particles can be accelerated by equipments called particle accelerators, where the particle gains kinetic energy while going through an variable electric potential. The cyclotron is a compact accelerator characterized by spiral particle trajectory (Kaplan, 1978). It was created with the purpose of speeding up various ions, supported by distinct electromagnetic power and technologies. Indeed, the final kinetic energy depends on the design, the mechanical structure and equipment materials. Its application scope varies ranging from nuclear physics research to the production of radioisotopes for medical diagnosis and to heavy ion beam extraction for therapy.

The technique grew out of the need to maximize the effectiveness of the treatment of tumors with minimal radiation damage to healthy tissues. The proton therapy was proposed by Robert Wilson in 1946, when there were already able to supply high energy proton beams at a level enough to 10 up to 25 cm penetration in internal tissues of the human body (Rêgo and Carlson, 2008).

The protons have a roughly rectilinear path with low energy deposition at its path and greater ionization in a narrow range near the end of the particle path followed by a sudden dropped of energy deposition (Bragg peak – Fig. 1) (Burigo, 2011). The penetration range of the beam and the maximum energy deposition will only depend on the initial energy of the incident particle. (Christóvão and Campos, 2010).

For this technique is required large particle accelerators which hinders the implementation of Proton Therapy Centers in some countries, such as Brazil, due to the need for an investment of tens of millions of dollars. However, Brazil will face it soon due to the gold radiation therapy standard for various neoplasia.

This study is a proposal that makes the proton therapy more accessible to the public. It is an alternative project of an electromagnetic unit equivalent to a proton circular accelerator to be coupled to the cyclotrons of radiopharmaceutical producers.

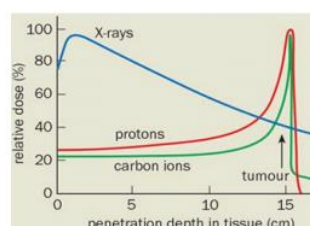


Figure 1. Dose distribution for carbon and protons, X-rays
 Source:(Rego; Carlson, 2008)

Herein, there were reports about the analytical calculations of the accelerator physical parameters related to the proton beam transport; the geometric design; the simulations of proton beam at the accelerator based on the ion transport in EMF CST (Computer Simulation Technology); and equipment modeling using AutoCAD.

2. MATERIALS AND METODS

2.1 Short description

At the initial stage, the analytical parameters associated with the protons trajectory is parsed by following the equations 1 to 6. Some of these equations satisfy the classical mechanics. However, some corrections must be made since, when the particle approaches the 2% of the speed of light, relativistic effects must be accounted for. The acceleration time and particle velocity on the acceleration process were obtained from simulation in CST software (Computer Simulation Technology).

Consider a proton with charge q_p and rest mass m_0 , emitted by a ion source. It is initially accelerated at a cyclotron to an initial energy E_0 equal to 15 MeV. This proton beam must pass several times by a unit of acceleration to reach kinetic energies of up to 64 MeV.

Through the classical physics, this unit is described in a simplified way as composed of two regions: a region of the recicular movement, where there is a uniform magnetic field \mathbf{B} ; and a region where acceleration is performed by an electric field \mathbf{E} . Both regions are engaged and distinct. The particle enters initially in the acceleration, where the magnetic field \mathbf{B} is null and the electric field \mathbf{E} is constant, with a speed v_0 . When it passes by this acceleration cavity the particle gains more power and increase its speed. The particle traverses the interior of the acceleration cavity in a time t_d . Then comes out with a v speed, as shown in Fig. 2, and returns to the starting point after completing a circular round with radius R at a time t_f (outside the region of acceleration). As its movement is perpendicular to a uniform magnetic field, the particle will describe a circular path in the region outside the structure of the acceleration. The higher the speed and the energy of the particle, the greater the radius R of the curvature.

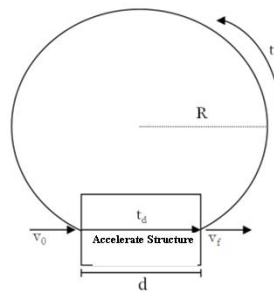


Figure 2. Particle path schema inside the acceleration device.
Source: Rabelo, 2012

2.2 Physical formulation at circulation region

Considering a proton with a speed v perpendicular to the magnetic field \mathbf{B} , the particle will evolve to a circular trajectory, with centripetal force \mathbf{F} acting. This motion can be described by the Lorentz Equation:

$$\mathbf{F} = m_0 \mathbf{a} = q_p B v \quad (1)$$

where m_0 is the mass of particle acceleration, q_p the charge particle, and Bv is the product of the magnetic field \mathbf{B} and module of speed v . The force and magnetic field vectors are perpendicular.

It is known that the acceleration vector a module is given by the formula:

$$a = \frac{v^2}{R} \quad (2)$$

It is possible to calculate the radius R of the circular trajectory of the proton, at each lap, replacing (2) into (1). The value of radius R will be assessed by:

$$R = \frac{p}{q_p B} \quad (3)$$

where p is the module of the relativistic particle momentum, mv . In terms of kinetic energy E_c , the non-relativistic momentum p is addressed as follows:

$$p = \sqrt{2m_0E_c} \tag{4}$$

And, the relativistic momentum p_r can be found by Eq. (5):

$$p_r = \frac{1}{c} \sqrt{E_c^2 + 2E_cm_0c^2} \tag{5}$$

where E_c is the kinetic energy of the particle. Substituting Eq. (4) into (3) or to the relativistic beam, i.e. (5) in (3), the relativistic radius R_r^i to the i^{th} turns shall be is :

$$R^i = \frac{\sqrt{2m_pE_c^i}}{q_pB}, \text{ or } R_r^i = \frac{p_r^i}{q_pB}, \text{ for } i = 1, \dots, n; \tag{6}$$

where R^i and R_r^i are the classical and relativistic radius of curvature of the particle in an orbit i^{th} . .

2.3 Acceleration region

The time and speed within the framework of acceleration were generated by the numerical CST code in the simulation of the trajectory of the beam passing through the electromagnetic fields, taking into account a real acceleration cavity.

2.4 Accelerator design and modified trajectory

The acceleration region was defined as a cylindrical cavity, coupled to magnets which hold circular particle trajectories with a common tangential point. This magnetic region is separated were splitted in two parts, in which the acceleration cavity is allocated. So, all particles (with smaller and larger energy) travel the same distance within the acceleration cavity, positioned in the middle of two "Dees". Thus, the relativistic particles spend different times along its path, and then come out in different time/phase. In order to compensate for this time discrepancies, the synchronization of the particle entering at the acceleration cavity is required to match an ideal electric field phase. The solution was to "delay" the particle in the magnet region by increasing the distance of the route, through an increasing in the linear trajectory coupled to the circular motion of the particle. This "delay" is done in areas where the magnetic field is reduced to close zero. The variation of magnetic field at the magnet is provided by slabs of material that carry the particle passage at areas in which the magnetic field lines were deviated..

The separation of the "Dees" in the central region has the same length of the acceleration cavity. At these dimensions, the low energy particle enters at the cavity into position and inclination, as seen in Fig. 3 (a).

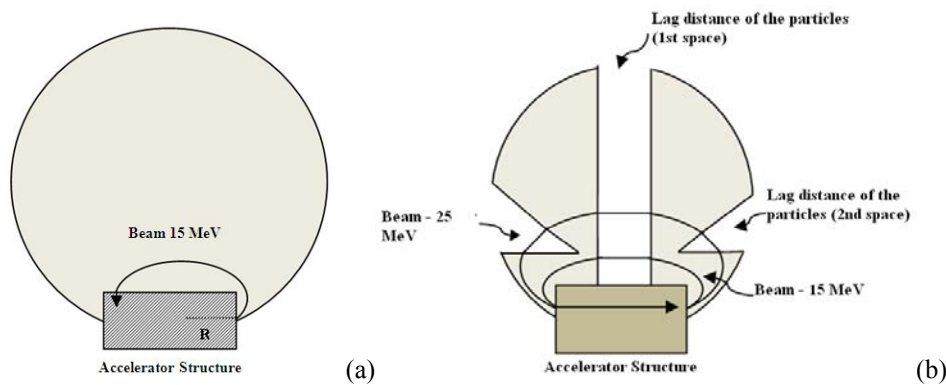


Figure 3. Possible trajectory of the first beam (a) without the detour and two beams of different energies (b) deviations.

Let us define t_d^i the time spent by the particle in the “Dees” gap L as follows:

R, A. Luísa and P, R, C. Tarcísio
Circular Accelerator Therapy

$$t_d^i = \frac{L}{v^i} \quad (7)$$

where L is the “dees” separation distance equal to 20 cm, and v speed (obtained from CST) for each beam kinetic energy E_c at the i^{th} turn.

Taken the initial speed of the particle, its travelling spent time through the acceleration cavity and the gap between “Dees”, at the first turn ($i=1$); the total time at the next turn T_t^i is calculated by:

$$T_t^i = T_{CST} + \frac{\pi R}{v} + t_d^1 + \frac{\pi R}{v} \quad (8)$$

where T_{CST} is the time required to cross the acceleration cavity, provided by CST simulations, πR the route accounting to each “Dee”, and t_d^1 the time spent at the “Dees” gap at the i^{th} turn.

To find out how long a particle beam is earlier than the other, their respective total times is subtracted of the first time at the particle enter in the accelerator at initial kinetic energy E_c^1 .

$$\Delta t^i = (T_t^i - T_t^1), \quad (9)$$

with the time values evaluated by Eq.8.

The differential time values shall be compensated by additional travelling distances required to each proton in order to delay its arrival at the acceleration cavity so that synchronism is achieved. The Eq. 10 provides the additional travelling distance dx^i associated to the i^{th} turns, such that:

$$dx^i = v^i \cdot \Delta t^i \quad (10)$$

To check, calculate the time t_d^i that the particle beam with velocity v^i spends to traverse the distance dx^i found by Eq. 10. Then add up all times to complete a turn: at the cavity, at the dees, and at the gaps. The Eq.9 calculation was rebuilt to meet the total time for all beam traverses the full trajectory of the accelerator, including delay distances. From the results it is possible to define the ideal geometry of the accelerator (Fig. 3-b).

3. RESULTS

Simulations have been performed based on the physical parameters presented on Tab. 1. Considering 15MeV as initial kinetic energy, Table 2 presents the number of laps, radius, linear momentum, speed and energy gain at the turn, in order to achieve final kinetic energy of 64 MeV, taken at the initial and final condition. Those were obtained from Eq. 1 to 6.

Table 1. Physical parameters addressed in the particle acceleration project..

Proton mass	$1,67 \times 10^{-27}$ kg
Proton charge	$1,6 \times 10^{-19}$ C
Potential difference between the electrodes	200 kV
Magnetic Field	3 T
Speed of light	3×10^8 m/s
Distance between electrodes	0,2 m
Initial kinetic energy	15 MeV

Table 2. Analytical calculated values related to proton trajectory at acceleration structure.

Kinetic energy (MeV)	15	64
Kinetic energy (Joules)	$2,40 \times 10^{-12}$	$1,02 \times 10^{-11}$
Number of laps	1	248
Radius (m)	0,18	0,38
Linear momentum (kg.m/s)	$8,96 \times 10^{-20}$	$1,85 \times 10^{-19}$
Relativistic linear momentum (kg.m/s)	$9,0 \times 10^{-20}$	$1,88 \times 10^{-19}$
Speed (m/s)	$5,36 \times 10^7$	$11,0 \times 10^7$

Relativistic speed (m/s)	$5,29 \times 10^7$	$10,5 \times 10^7$
Speed at accelerator cavity from CST (m/s)	$5,29 \times 10^7$	$10,5 \times 10^7$
Kinetic energy gain (keV) at the turn	157	93
Relativistic mass (kg)	$2,03 \times 10^{-27}$	$2,65 \times 10^{-27}$

Figure 4 (a) and (b) show the passage of the particle beam by acceleration cavity. The CST simulates the beam energy gain, in each turn, from 15 MeV to 64 MeV, respectively.

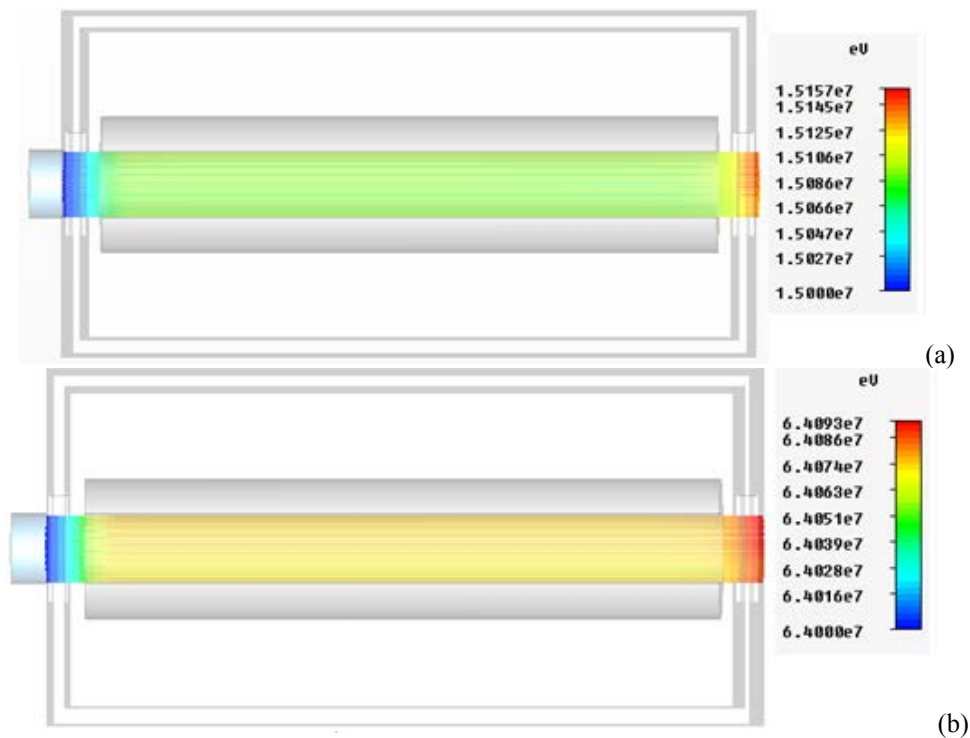


Figure 4. Proton beam acceleration with kinetic energy at 15 MeV (a) and 64 MeV (b).

The spending time at the acceleration cavity in function of the proton kinetic energy at the turn i^{th} , addressed in the CST, was presented at Fig. 5, where T_i is the initial time, T_m is the time that accounts for the beam reaching half of the acceleration and T_f the time taken to traverse the entire region.

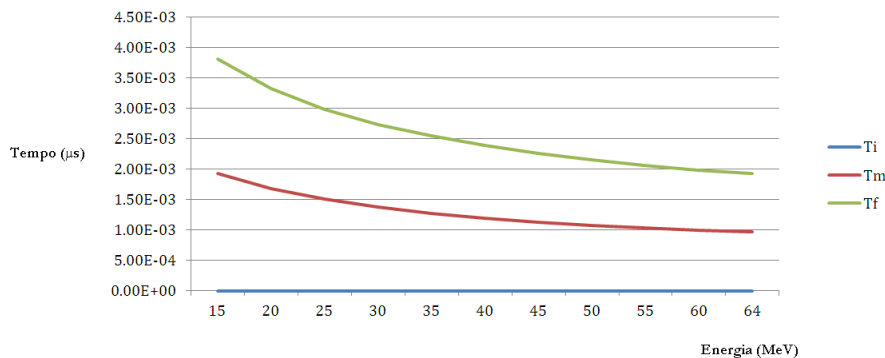


Figure 5. Proton trajectory times to cross the acceleration cavity versus kinetic energy,

From Eq. 7, the time delay at i^{th} turn were found and expressed at Table 3.

Table 3. Speed and time at the i^{th} turns.

Kinetic energy (MeV)	Speed (m/s)	Time in i^{th} turn (s)
15	$5,29 \times 10^7$	$3,78 \times 10^{-9}$
20	$6,12 \times 10^7$	$3,27 \times 10^{-9}$
25	$6,83 \times 10^7$	$2,93 \times 10^{-9}$
30	$7,42 \times 10^7$	$2,70 \times 10^{-9}$
35	$8,00 \times 10^7$	$2,50 \times 10^{-9}$
40	$8,50 \times 10^7$	$2,35 \times 10^{-9}$
45	$8,90 \times 10^7$	$2,25 \times 10^{-9}$
50	$9,40 \times 10^7$	$2,13 \times 10^{-9}$
55	$9,80 \times 10^7$	$2,04 \times 10^{-9}$
60	$10,2 \times 10^7$	$1,96 \times 10^{-9}$
65	$10,5 \times 10^7$	$1,90 \times 10^{-9}$

Then, suming up the time spent on the first detour to time spent to pass in semicircles, according to Eq. 8, were shown in Table 4.

Table 4. Travelling proton time from the circulation and the delay time.

Kinetic energy [MeV]	Delay time "Dees"[s]	Total time [s]
15	$2,23 \times 10^{-8}$	$2,99 \times 10^{-8}$
20	$2,24 \times 10^{-8}$	$2,90 \times 10^{-8}$
25	$2,24 \times 10^{-8}$	$2,83 \times 10^{-8}$
30	$2,26 \times 10^{-8}$	$2,81 \times 10^{-8}$
35	$2,27 \times 10^{-8}$	$2,77 \times 10^{-8}$
40	$2,28 \times 10^{-8}$	$2,76 \times 10^{-8}$
45	$2,32 \times 10^{-8}$	$2,75 \times 10^{-8}$
50	$2,32 \times 10^{-8}$	$2,74 \times 10^{-8}$
55	$2,33 \times 10^{-8}$	$2,74 \times 10^{-8}$
60	$2,34 \times 10^{-8}$	$2,74 \times 10^{-8}$
64	$2,35 \times 10^{-8}$	$2,73 \times 10^{-8}$

Table 5 shows the delay time required to synchronize the particle at each turn, and its conversion in distance, generated from Eq.8 to 11.

Table 5. The conversion of time delay in distance (dx) in the path of the beam at magnetic region.

Particle energy (MeV)	Δt^i (s)	dx^i (cm)
15	0	0
20	$-9,12 \times 10^{-10}$	-0,055
25	$-1,54 \times 10^{-9}$	-0,105
30	$-1,82 \times 10^{-9}$	-0,135
35	$-2,15 \times 10^{-9}$	-0,172
40	$-2,29 \times 10^{-9}$	-0,195
45	$-2,21 \times 10^{-9}$	-0,196
50	$-2,46 \times 10^{-9}$	-0,230
55	$-2,47 \times 10^{-9}$	-0,242
60	$-2,52 \times 10^{-9}$	-0,257
64	$-2,54 \times 10^{-9}$	-0,266

After synchronization, the total time spending by the proton in each turns was 2.99×10^{-8} s, as constant. Therefore, the particle trajectory at all kinetic energies, held similar time travelling. This constant time is required to match the frequency oscillation period, i.e., $f = 1/T \rightarrow f = 33.5$ MHz. Thus, all particles spend the same time to give a complete turn, regardless of their kinetic energy, and enter in the resonance cavity at the similar cycle.

Based on the analytical and simulation results, it was possible to design the equipment and set the ideal geometric and physical parameters. The Figs 6, 7 and 8 show the final design of the proton accelerator in AutoCAD.

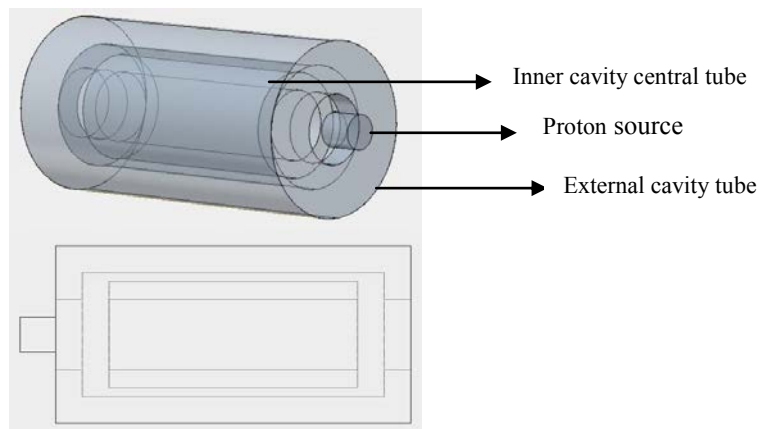


Figure 6. Acceleration structure and particle source.

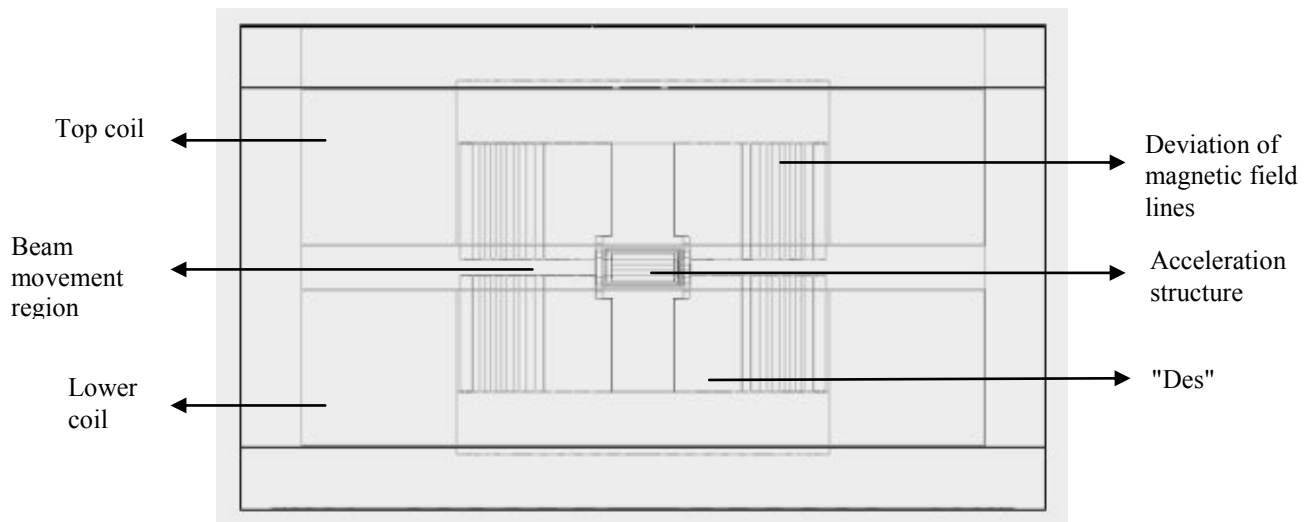


Figure 7. Ferromagnetic structure scheme.

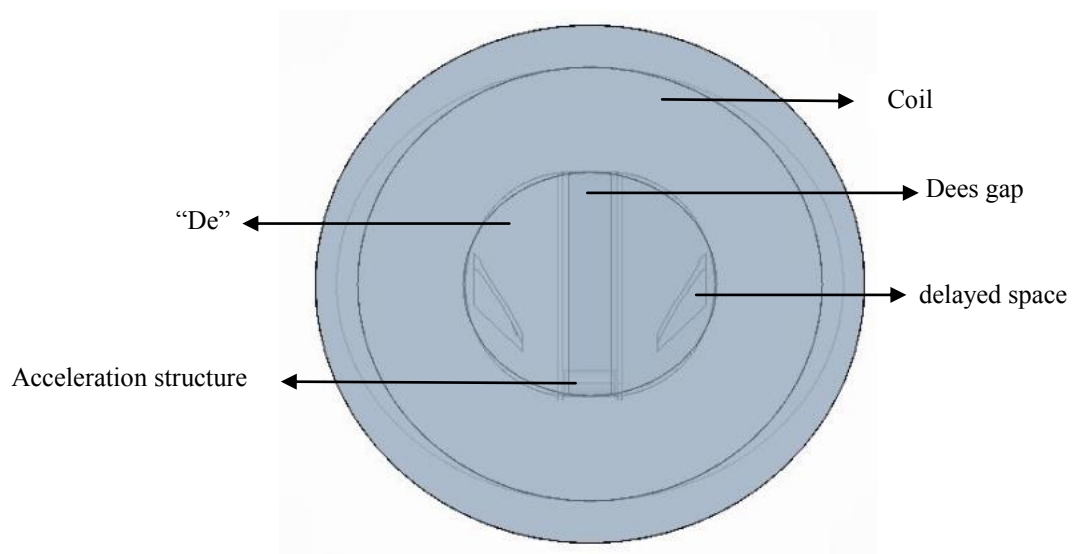


Figura 8. Planar representation of the Accelerator at the core Center.

R, A. Luísa and P, R, C. Tarcísio
Circular Accelerator Therapy

4. CONCLUSION

Herein, there were demonstrated the feasibility of developing a circular proton accelerator, that can be coupled to cyclotrons accelerators as Cyclone 30 of IPEN, or even PET trace CDTN accelerator, or private ones. Such accelerators meet the minimum kinetic energy of 15 MeV needed for feed the present equipment; however, initial kinetic energy may be adjusted.

This unit, with an initial kinetic energy of 15 MeV, provides 64 MeV protons with enough kinetic energy after 248 turns at 3 Tesla for the treatment of ocular tumor. The present study is encouraging, because the idea of attaching a unit of acceleration along with cyclotron FDG producer, can produce proton beams for therapy with low installation cost, providing condition to implement the proton therapy in Brazil. The possibility of having a 64 MeV proton accelerator in Brazil is of paramount social importance.

The idea and physical principles discussed in this study brings the possibility of developing the technology for domestic production, improving the quality of life in patients suffering from this type of illness, in addition to the scientific and technological development of the country in the area of radiation.

Further research can be done to extending this project to other purposes, including simulations to different kinetic energy of proton at other tracks.

5. ACKNOWLEDGEMENTS

CAPES and CNPq, FAPEMIG by institutional support and the NRI group.

6. REFERENCES

- Burigo, L.N., 2011. *Hadronterapia: Simulações da Contribuição de Processos Nucleares para o tratamento de tumores*. Dissertation, Universidade Federal do Rio Grande do Sul, RS - Brasil.
- Christóvão, M.T., Campos, T.P.R., 2010. "Análise da distribuição espacial de dose absorvida em próton terapia ocular." *Radiologia Brasileira*, Vol. 43, n 4, São Paulo. Scielo. Brazil
Mai. 2013<http://www.scielo.br/scielo.php?script=sci_arttext&pid=S0100-39842010000400009>
- Kaplan, I., 1978. *Física Nuclear*, 2 ed. Ed. Guanabara Dois, 636 p.
- Rabelo, L.A., 2012. *Projeto de acelerador circular para prótons para fins de teleterapia ocular*. Dissertation, Universidade Federal de Minas Gerais, MG – Brasil.
- Rêgo, M.E.M. and Carlson, B.V., 2008. "Reações Nucleares induzidas por Prótons em Isótopos com Uso na Radioterapia". In *Anais do 14º Encontro de Iniciação Científica e Pós-Graduação do ITA – XIV ENCITA*. São José dos Campos, SP, Brazil.

7. RESPONSIBILITY NOTICE

The author(s) is (are) the only responsible for the printed material included in this paper.